ZAG alleviates HFD-induced insulin resistance accompanied with decreased lipid depot in skeletal muscle in mice[S]

Shi-Xing Gao, Jun Guo, Guo-Qiang Fan, Yu Qiao, Ru-Qian Zhao, and Xiao-Jing Yang[1]

Key Laboratory of Animal Physiology and Biochemistry, Nanjing Agricultural University, Nanjing 210095, People's Republic of China

Abstract **Over the past two decades, intramuscular lipids have been viewed as a cause of insulin resistance due to their ability to suppress insulin-stimulated glucose uptake in skeletal muscle. Zinc-α2-glycoprotein (ZAG) is an adipokine involved in lipolysis of white adipose tissue (WAT). To investigate the action of ZAG on insulin resistance induced by a high-fat diet (HFD), which affects the intramuscular fat, mice were divided into three groups, normal diet, HFD, and ZAG treatment under HFD (HFZ). The results showed that the insulin sensitivity of ZAG-treated mice was significantly improved. The body weight, WAT weight, and intramuscular fat were significantly decreased in the HFZ group compared with the HFD group. The lipolytic enzymes, including phosphorylation of hormone-sensitive lipase and adipose triglyceride lipase, were significantly upregulated in the skeletal muscle of mice that received the ZAG treatment compared with the HFD group. Insulin signaling proteins, such as phosphorylation of insulin receptor substrate 1 and cell membrane glucose transporter type 4, were also significantly increased in the skeletal muscle of the ZAG-treated group. Furthermore, a metabolic rate study showed that ZAG overexpression increases the respiratory exchange ratio and heat production. In vitro, ZAG treatment promotes glucose uptake and decreases intracellular lipids in C2C12 myotubes.[F] Taken together, these data showed that overexpression of ZAG alleviates HFD-induced insulin resistance in mice, along with decreasing the lipid content of skeletal muscle.**—Gao, S-X., J. Guo, G-Q. Fan, Y. Qiao, R-Q. Zhao, and X-J. Yang. **ZAG alleviates HFD-induced insulin resistance accompanied with decreased lipid depot in skeletal muscle in mice.** ***J. Lipid Res.*** **2018.** 59: **2277–2286.**

Supplementary key words zinc-α2-glycoprotein • lipolysis • intramuscular fat

In recent years, insulin resistance has received considerable attention due to its major pathogenic role in the development of metabolic syndrome, which may result in diabetes, hypertension, etc. The causes of insulin resistance are complicated and may vary for different individuals. Nevertheless, the factor most commonly associated with insulin resistance is excess adiposity due to the increase in circulating fatty acids and ectopic lipids (1). Intramuscular lipids are an indispensable energy source for skeletal muscle. These lipids play pivotal roles in metabolism not only for skeletal muscle but also for the entire body. The accumulation of ectopic lipids in skeletal muscle is thought to be involved in the etiology of type II diabetes and insulin resistance by suppressing insulin-stimulated glucose uptake (2, 3). Skeletal muscle accounts for ∼80% of insulin-stimulated glucose uptake (4). It is the primary site of insulin-stimulated glucose uptake and metabolism (4, 5). Earlier studies, both in humans (6) and in animal models (7), indicated that intramuscular lipid accumulation was associated with insulin resistance, thereby providing a potential link between dysregulated fatty acid metabolism in skeletal muscle and insulin resistance (6–9).

Zinc-α2-glycoprotein (ZAG) is a 43 kDa soluble glycoprotein, first isolated from human plasma. However, a previous study showed that ZAG was produced in many tissues,

This study was supported by National Natural Science Foundation of China Grant 31572482, National Key Research and Development Program of China Grant 2016YFD0500502, and the Priority Academic Program Development of Jiangsu Higher Education Institutions.

Manuscript received 29 November 2017 and in revised form 24 September 2018.

Published, JLR Papers in Press, October 14, 2018
DOI https://doi.org/10.1194/jlr.M082180

Abbreviations: AKT, protein kinase B; ATGL, adipose triglyceride lipase; BAT, brown adipose tissue; β2-AR, β-adrenoreceptor 2; β3-AR, β-adrenoreceptor 3; C/EBPβ, CCAAT/enhancer binding protein β; Glut4, glucose transporter type 4; GTT, glucose tolerance test; HDLc, HDL cholesterol; HFD, high-fat diet; HFZ, ZAG treatment under high-fat diet; HOMA-IR, homeostatic model assessment of insulin resistance; HSL, hormone-sensitive lipase; INSR, insulin receptor; IRS1, insulin receptor substrate 1; ITT, insulin tolerance test; LDLc, LDL cholesterol; M-Glut4, cell membrane glucose transporter type 4; ND, normal diet; p-AKT, phosphor-S473 of protein kinase B;PGC1α, peroxisome proliferator-activated receptor γ coactivator 1α; p-HSL, phosphor-S855 of hormone-sensitive lipase; p-IRS1, phosphor-S307 of insulin receptor substrate 1; PKA, protein kinase A; p-PKA, phosphor-T197 of protein kinase A; RER, respiratory exchange ratio; rZAG, recombinant zinc-α2-glycoprotein; TG, triglyceride; UCP, uncoupling protein; VCO2, carbon dioxide production; VO2, oxygen consumption; WAT, white adipose tissue; ZAG, zinc-α2-glycoprotein.

[1] To whom correspondence should be addressed.
e-mail: yangxj@njau.edu.cn

[S] The online version of this article (available at http://www.jlr.org) contains a supplement.

including brown adipose tissue (BAT), white adipose tissue (WAT), and the liver (10). Until now, the known biological role of ZAG has been as a lipid-mobilizing factor in WAT. ZAG stimulates lipolysis in isolated mouse and human adipocytes and reduces body fat in both normal and obese (ob/ob) mice (11). Several studies point to ZAG as a possible candidate gene for body weight regulation because transgenic mice overexpressing ZAG exhibit weight loss (12), whereas ZAG-deficient mice experience obvious weight gain (13). Moreover, the lipolytic effect of ZAG in adipose tissues has been attributed to the activation of β-adrenoreceptor 3 (β3-AR) and upregulation of cAMP via the β3-AR/cAMP pathway (14).

Though it is known that ZAG influences the lipid metabolism of WAT, its effects on intramuscular fat have never been reported. A previous limited study showed that treatment with ZAG decreases body weight and improves insulin sensitivity in ob/ob mice (15). However, the underlying mechanism is still largely unknown.

In the present study, we aimed to investigate the role of ZAG in regulating intramuscular fat and its possible action on insulin sensitivity, in an attempt to further clarify the function of ZAG in metabolism and provide a potential target for preventing insulin resistance.

MATERIALS AND METHODS

Ethics statement

Experiments were conducted in accordance with the guidelines of the Animal Ethics Committee of Nanjing Agricultural University, China. Euthanasia and sampling procedures complied with the "Guidelines on Ethical Treatment of Experimental Animals" (2006) No. 398, published by the Ministry of Science and Technology, China, and with the "Regulation regarding the Management and Treatment of Experimental Animals" (2008) No. 45, published by the Jiangsu Provincial People's Government.

Animals and diets

Four-week-old specific pathogen-free C57BL/6J (12–14 g) male mice were purchased from the Animal Core Facility of Nanjing Medical University. The animals were accommodated four per cage and housed in a controlled environment (40–60% relative humidity and constant temperature, 22–24°C) with a 12 h light/12 h dark cycle, and allowed to adapt to their environment for 1 week. After the adaptation period, the mice were randomly assigned to two groups; one group was fed a normal diet (ND; 10% fat) and the other was fed a high-fat diet (HFD; 45% fat) for 9 weeks to establish obesity. The nutrients of the ND and HFD are listed in **Table 1**. HFD-induced obese mice were further divided into two subgroups; the HFD group and the HFD with ZAG overexpression group (HFZ). ZAG recombinant plasmid (25 μg) or pcDNA 3.1 negative control plasmid, in 150 μl OPTI-MEM medium, was mixed thoroughly with 40 μl of Lipofectamine 2000 in 150 μl of OPTI-MEM medium, and the resulting 300 μl mixture was incubated at room temperature for 30 min. Then, the HFZ group mice were treated by intravenous administration into the tail vein with ZAG recombinant plasmid, while mice in the ND and the HFD groups received pcDNA 3.1. This treatment was given eight times, once every 3 days. The dose and route of administration were chosen based on previous report (12).

TABLE 1. The nutrients of 10% fat and 45% fat of diets

	10% Fat	45% Fat
Energy composition	100	100
Protein (%)	20	20
Carbohydrate (%)	70	35
Fat (%)	10	45
Composition of fatty acid	100	100
Saturated (%)	28.7	40.3
Monounsaturated (%)	32.7	40.4
Polyunsaturated (%)	38.6	19.3
Type of fat (gm)	45	202.5
Lard (g)	20	177.5
Soybean oil (g)	25	25

Blood and tissue sample collection

Two days after the eighth treatment, all mice were fasted for 8–10 h before sampling. Mice were anesthetized with an intraperitoneal injection of pentobarbital sodium (80 mg/kg) and blood was collected from the abdominal aorta using a syringe with heparin (100 IU/ml). The gastrocnemius muscle and plasma were harvested and stored at −80°C pending analysis. The percentages of epididymal and perinephric fat were calculated by dividing the body weight of the mice by the epididymal fat mass or the perinephric fat mass, respectively.

Biochemical analysis and glycogen assay

Concentrations of glucose, triglycerides (TGs), total cholesterol, HDL cholesterol (HDLc), LDL cholesterol (LDLc), and NEFAs were detected with the automatic biochemical analyzer, Hitachi 7020 (HITACHI, Ltd., Japan), using commercial assay kits 995-18311, 995-33093, 999-33493, 998-09011, 993-39993, and 995-09901 (Wako Pure Chemical Industries, Ltd., Japan), respectively. Muscle concentrations of TGs and NEFAs were detected using commercial assay kits 995-33093 and 995-09901 (Wako Pure Chemical Industries, Ltd.), respectively. The plasma concentration of insulin was measured by Luminex 200 (no. CNBMSLX200; China Biomarker Service), using Magnetic Bead MAPmate (Merck and Millipore, Germany) according to the instructions provided by the manufacturer.

TSE PhenoMaster system

In the present study, individually housed mice (n = 5 from each group) were continuously monitored for physiological parameters and basal behaviors, including oxygen consumption (VO2), carbon dioxide production (VCO2), respiratory exchange ratio (RER), energy expenditure, body weight, cumulative food intake, and total locomotor activity by the TSE PhenoMaster system (TSE Systems China, Germany) at ambient room temperature (22–24°C).

RNA isolation and quantitative real-time PCR analysis

Total RNA from gastrocnemius muscle (n = 8 per group) was extracted using TRIzol reagent (Invitrogen, USA) and reverse transcribed with the PrimeScript first strand cDNA synthesis kit (RR048A; Takara Bio Inc., Japan). All the procedures were performed according to the manufacturers' protocols. Primers were synthesized by Generay Biotech (Shanghai, China). Real-time PCR was performed using the Mx3000P QPCR system (Stratagene, USA). All data were normalized to β-actin as internal control and quantitative measurements were obtained using the 2-ΔΔCt method.

Western blot and quantification

Protein concentrations from all samples were measured using the BCA-kit (Thermo Scientific, USA), followed by protein concentration normalization, before all Western blot experiments. Membrane proteins were extracted by the Mem-PER Plus membrane protein extraction kit (89842; Thermo Scientific). This kit enables small-scale solubilization and enrichment of integral membrane proteins and membrane-associated proteins in a simple reagent-based procedure. Western blot was carried out following standard procedure and final band intensity (QL-BG) was quantified using BioPix iQ22. All data were normalized to background and loading control. Primary antibodies used and their sources were as follows: ZAG (ab117275; Abcam, USA), protein kinase A (PKA) (BS2648; Bioworld Technology, Inc., USA), phosphor-T197 of PKA (p-PKA) (BS4345; Bioworld Technology, Inc.), adipose TG lipase (ATGL) (BS7989; Bioworld Technology, Inc.), hormone-sensitive lipase (HSL) (BS2742; Bioworld Technology, Inc.), phosphor-S855 of HSL (p-HSL) (BS4234; Bioworld Technology, Inc.), glucose transporter type 4 (Glut4) (sc53566; Santa Cruz Biotechnology, USA), insulin receptor substrate 1 (IRS1) (BS3589; Bioworld Technology, Inc.), phosphor-S307 of IRS1 (p-IRS1) (BS4725P; Bioworld Technology, Inc.), protein kinase B (AKT) (ab32505; Abcam), phosphor-S473 of AKT (p-AKT) (ab81283; Abcam), peroxisome proliferator-activated receptor γ coactivator 1α (PGC1α) (sc-13067; Santa Cruz Biotechnology), mitochondrial uncoupling protein (UCP)3 (BS2849; Bioworld Technology, Inc.), CCAAT/enhancer binding protein β (C/EBPβ) (sc-150x; Santa Cruz Biotechnology), FASN (BS2948P; Bioworld Technology, Inc.), and β-actin (AP0063; Bioworld Technology, Inc.).

Assays of HSL concentrations

HSL concentrations were assayed using an enzyme-linked immunosorbent assay kit (SEB276Mu; Cloud-Clone Corp., China). Tissues and cells were prepared in ice-cold PBS before homogenization. The tissues were minced to small pieces and homogenized in fresh lysis buffer (IS007; Cloud-Clone Corp.) with a glass homogenizer on ice (1:20, w:v). Cells were shaken and collected in a cell culture 6-well plate with 150 μl of fresh lysis buffer (IS007; Cloud-Clone Corp.). The resulting suspension was sonicated with an ultrasonic cell disrupter until the solution was clarified. Then, the homogenates were centrifuged for 5 min at 10,000 *g* and the supernatants were collected. The assay procedures were operated according to the manufacturer's instructions.

Glucose and insulin tolerance tests

Glucose tolerance tests (GTTs) and insulin tolerance tests (ITTs) were performed as previously described (16, 17). Intraperitoneal GTTs were performed in 6 h-fasted mice. Glucose (G7021; Sigma, USA) was injected intraperitoneally and blood samples were obtained from the tail tip after 0, 15, 30, 45, 60, 90, and 120 min. The glucose dose used during these tests was 2 g/kg body weight. Blood glucose levels were measured by glucometer (Accu-check Advantage II monitor; Roche Diagnostics, Australia). Prior to performing ITTs, the mice were fed ad libitum. After determination of basal blood glucose concentrations, each mouse received an intraperitoneal injection of insulin (0.75 IU/kg body weight, Actrapid; Novo Nordisk, Denmark) and glucose concentrations in blood were measured after 15, 30, 45, and 60 min.

Cell experimental

C2C12 myotubes were cultured in growth medium composed of DMEM and 10% fetal bovine serum supplemented with penicillin (100 units/ml) and streptomycin (100 μg/ml). Once they reached confluence, the cells were switched to a differentiation medium composed of DMEM supplemented with 2% horse serum. Sodium oleate (Sigma) and sodium palmitate (Sigma) were conjugated to fatty acid-free BSA. Briefly, sodium palmitate was dissolved in NaOH (0.05 M) solution prepared in PBS and dissolved at 80°C for about 10–15 min with periodic vortexing; while sodium oleate is dissolved in PBS alone and dissolved at 60°C for about 10–15 min with periodic vortexing. Both fatty acids were produced to 50 mM stock solutions. To obtain a 5 mM oleate-palmitate stock solution, each 50 mM of fatty acid solution was added dropwise to BSA solution (18.3% w/v, dissolved in DMEM) at an equimolar 2:1 ratio. Prior to treatment, differentiation medium was used to produce fatty acid mixtures at 1.0 mM concentrations. The cells were differentiated for 2 days before treatment with 1.0 mM oleate-palmitate solution or BSA alone as control for a period of 4 days. Medium was changed every 2 days. Then, the cells were switched to a standard differentiation medium without fatty acid and phenol red, and treated with recombinant ZAG (rZAG, 1 μg/ml) (18, 19) or PBS alone as control for 12 h. Then, cell media were collected to test glucose concentration and cells were collected to test TG, NEFA, and HSL contents.

Statistical analysis

Data were statistically analyzed using the SPSS software 19.0, Microsoft Excel, and GraphPad Prism 6.0. All data are presented as the mean ± SEM. One-way ANOVA was used to evaluate the statistical significance of differences among the three groups. In the figures and tables, different letters denote a significant difference between two groups, as determined. Statistical significance was defined as $P < 0.05$. The 2-ΔΔCt method was applied to analyze real-time PCR data. The number of replicates used for statistics are noted in the tables and figures.

RESULTS

ZAG reduces body weight and decreases fat mass

ZAG treatment observably reduced body weight (**Fig. 1A–**C) and decreased the size of the fat mass (Fig. 1A) and adipose cells (Fig. 1A). The consumption of the HFD and HFZ groups' diet was significantly lower ($P < 0.05$) than the control group, and there was no difference between the HFD group and the HFZ group during the ZAG recombinant plasmid treatment period (Fig. 1D). The epididymal fat weight and perinephric fat weight were significantly reduced ($P < 0.05$, Fig. 1E) in the HFZ group compared with the HFD group. Plasma TG concentrations showed no difference between the ND group and the HFD group, but they were higher in the HFZ group than in the HFD group (**Table 2**). Plasma NEFA, cholesterol, HDLc, and LDLc concentrations were significantly higher ($P < 0.05$) in the HFD group than the ND group, and were reduced ($P < 0.05$) by ZAG treatment compared with the HFD group (Table 2). In addition, the concentrations of TG and NEFA in gastrocnemius muscle were observably decreased ($P < 0.05$, Fig. 1F) in the HFZ group compared with the HFD group.

ZAG improves glucose tolerance and alleviates insulin resistance in HFD-induced obese mice

Following the ZAG recombinant plasmid treatment, we examined glucose uptake and insulin sensitivity by performing GTTs and ITTs on mice. The results indicated

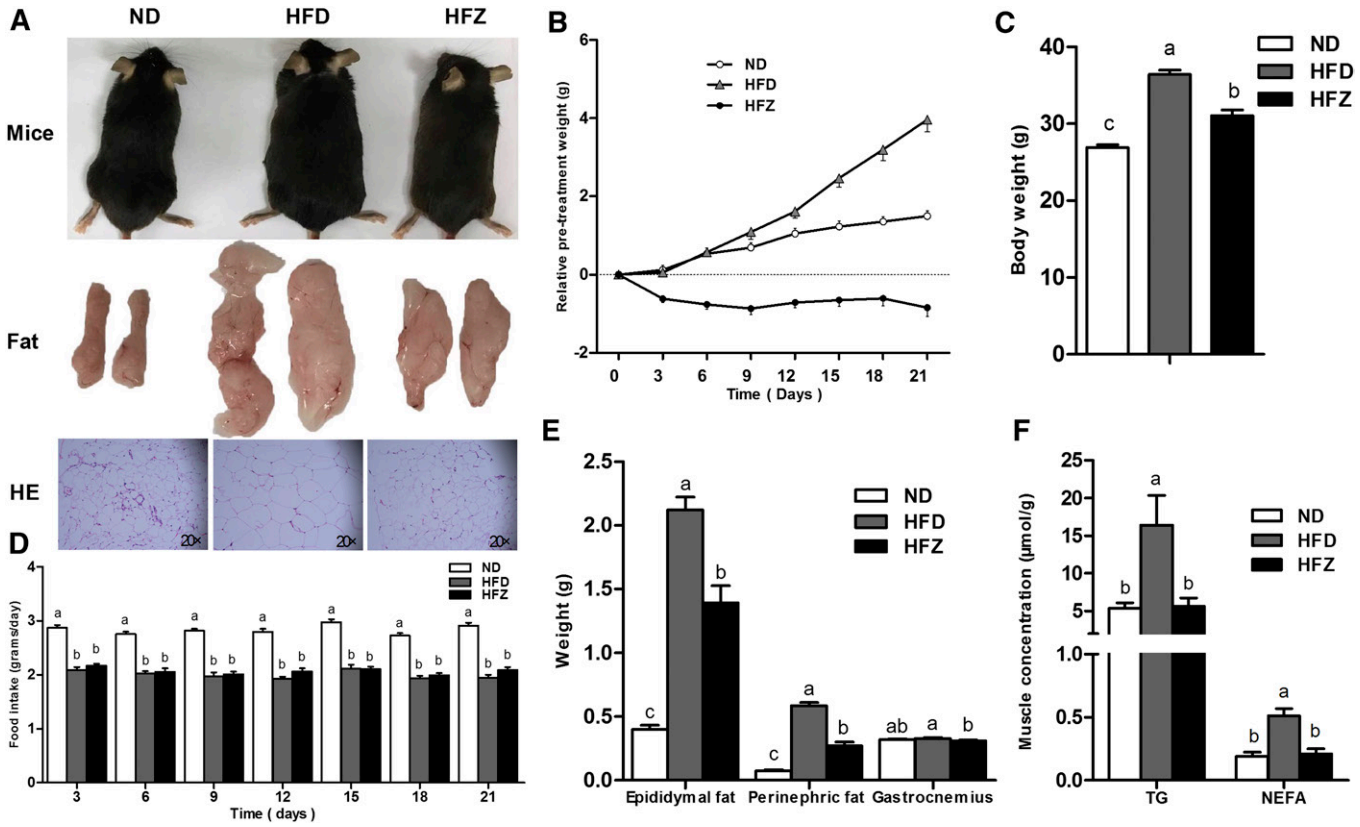

Fig. 1. ZAG overexpression reduces body weight and alleviates obesity. A: Three phenotypes of mice, epididymal fat mass and hematoxylin and eosin (HE) staining (n = 3 per group) of epididymal fat tissue from the ND group, the HFD group, and the HFZ group. B: Changes in body weight over the ZAG recombinant plasmid treatment period. Body weight (C) and epididymal fat weight, perinephric fat, weight, and gastrocnemius muscle weight (E) of mice from the three groups (n = 8 per group). D: Food intake during ZAG recombinant plasmid treatment period. F: Concentrations of TG and NEFA in gastrocnemius muscle of mice from the three groups (n = 8 per group). The ND group was fed with ND, whereas the HFD and HFZ groups were fed with HFD. The results are expressed as mean ± SEM. Different letters indicate significant differences between groups ($P < 0.05$). Error bars indicate SEM.

that ZAG significantly alleviated glucose intolerance and insulin resistance in the HFZ group compared with the HFD mice (**Fig. 2A**, B). Insulin plasma concentration was significantly ($P < 0.05$) elevated in the HFD group compared with the ND group, and ZAG treatment significantly decreased it in the HFZ group compared with the HFD group (Fig. 2D). Although the plasma concentration of glucose was not different between the HFD group and the HFZ group (Fig. 2C), the value obtained using the homeostatic model assessment of insulin resistance (HOMA-IR) was significantly lower in the HFZ group compared with the HFD group (Fig. 2E).

ZAG changes the insulin signaling pathway in skeletal muscle

To gain a better understanding of the role of ZAG in the insulin signaling pathway, we examined the mRNA of related genes, as well as protein expression levels in gastrocnemius muscle. The mRNA expression of insulin receptor (INSR), IRS1, Glut1, and Glut4 was significantly higher ($P < 0.05$) in the HFZ group compared with the HFD group (**Fig. 3A**). No difference in AKT mRNA expression was observed between the HFZ group and the HFD group (Fig. 3A). Although the total protein levels of IRS1 and AKT showed no difference between the three groups, the phosphorylation levels of IRS1 and AKT were observably higher ($P < 0.05$) in the HFZ group compared with the HFD group (Fig. 3B, C). Based on these findings, we detected total Glut4 and cell membrane Glut4 (M-Glut4) protein levels. The results indicate no obvious changes in total Glut4 among the three groups, but M-Glut4 was significantly higher ($P < 0.05$) in the HFZ group compared with the HFD group (Fig. 3D). These data demonstrate that

TABLE 2. The biochemical parameters in plasma

Parameters	ND	HFD	HFZ
TG (mmol/l)	0.61 ± 0.07b	0.50 ± 0.04b	1.01 ± 0.07a
NEFA (μmol/l)	685.4 ± 45.82b	861.1 ± 33.09a	544.0 ± 40.02c
Cholesterol (mmol/l)	2.84 ± 0.05c	4.02 ± 0.06a	3.15 ± 0.07b
HDLc (mmol/l)	2.23 ± 0.05b	3.00 ± 0.05a	2.31 ± 0.05b
LDLc (mmol/l)	0.28 ± 0.01c	0.76 ± 0.02a	0.58 ± 0.03b

The letters a, b, and c indicate significant differences between groups, as determined ($P < 0.05$).

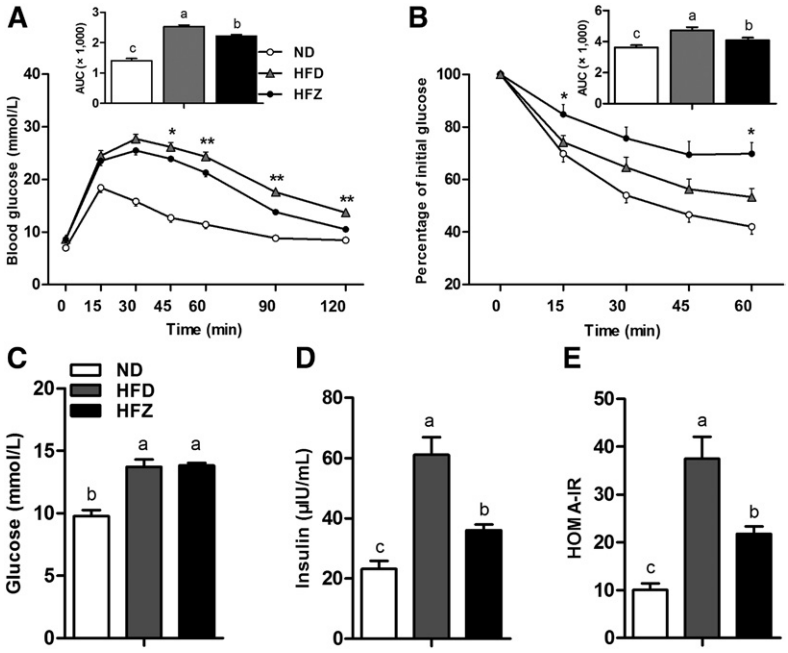

Fig. 2. ZAG overexpression improves glucose tolerance and combats insulin resistance. GTT (A) and ITT (B) in ND mice, obese mice fed HFD, and ZAG overexpression mice fed HFD (n = 8 per group). Glucose concentration (C) and insulin concentration (D) in plasma and HOMA-IR (E) for the three groups (n = 8 per group). Values are expressed as mean ± SEM. *$P <$ 0.05, **$P < 0.01$. Different letters indicate significant differences between groups, as determined ($P < 0.05$). Error bars indicate SEM.

ZAG overexpression affects the insulin signaling pathway in skeletal muscle under a HFD.

ZAG increases lipolysis via the β-AR/cAMP/PKA pathway in skeletal muscle

To further examine the function of ZAG in lipolysis, we studied the β-AR/cAMP/PKA pathway in skeletal muscle. The results show that ZAG plasma concentration was lower ($P < 0.05$) in the HFD group than in the ND group, and was significantly increased ($P < 0.05$) by the ZAG treatment (**Fig. 4A**). Furthermore, we found that the β3-AR mRNA and protein expression levels were significantly increased ($P < 0.05$) in the HFZ group compared with the HFD group (Fig. 4B, C). Although the mRNA level of β-adrenoreceptors 2 (β2-ARs) showed no difference between the three groups, the protein level of β2-AR was significantly increased ($P < 0.05$) in the HFZ group compared with the HFD group (Fig. 4B, C). The levels of p-PKA protein and the downstream proteins of HSL, p-HSL, and ATGL were also significantly higher ($P < 0.05$) in the HFZ group compared with the HFD group (Fig. 4D). In addition, the concentrations of HSL were increased ($P < 0.05$) by the ZAG treatment (Fig. 4E). The levels of the lipid synthesis proteins, C/EBPβ and FASN, showed no difference between the three groups (Fig. 4F). Moreover, the expression of key genes involved in mitochondrial thermogenesis, such as UCP3 and PGC1α, were examined in this study. The results show that both the mRNA and protein expression levels of PGC1α showed no differences between the three groups, yet the mRNA and protein expression of UCP3 were significantly increased ($P < 0.05$) in the HFZ group compared with the HFD group (Fig. 4G, H).

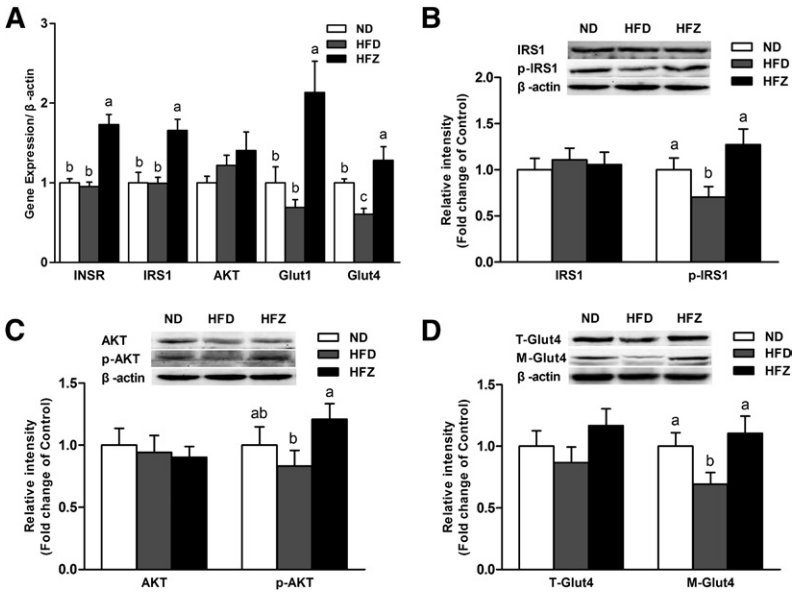

Fig. 3. ZAG overexpression changes the insulin signaling pathway in skeletal muscle. A: The mRNA expression levels of INSR, IRS1, AKT, Glut1, and Glut4 (A) (n = 6 per group). Western blot analysis revealed accumulation of IRS1 and p-IRS1 (B), AKT and p-AKT (C), and total Glut4 (T-Glut4) and M-Glut4 (D) in the gastrocnemius muscle of mice from the three groups (n = 6 per group). The ND group was fed with ND, whereas the HFD and HFZ groups were fed with HFD. Values are expressed as mean ± SEM. Different letters indicate significant differences between groups, as determined ($P < 0.05$). Error bars indicate SEM.

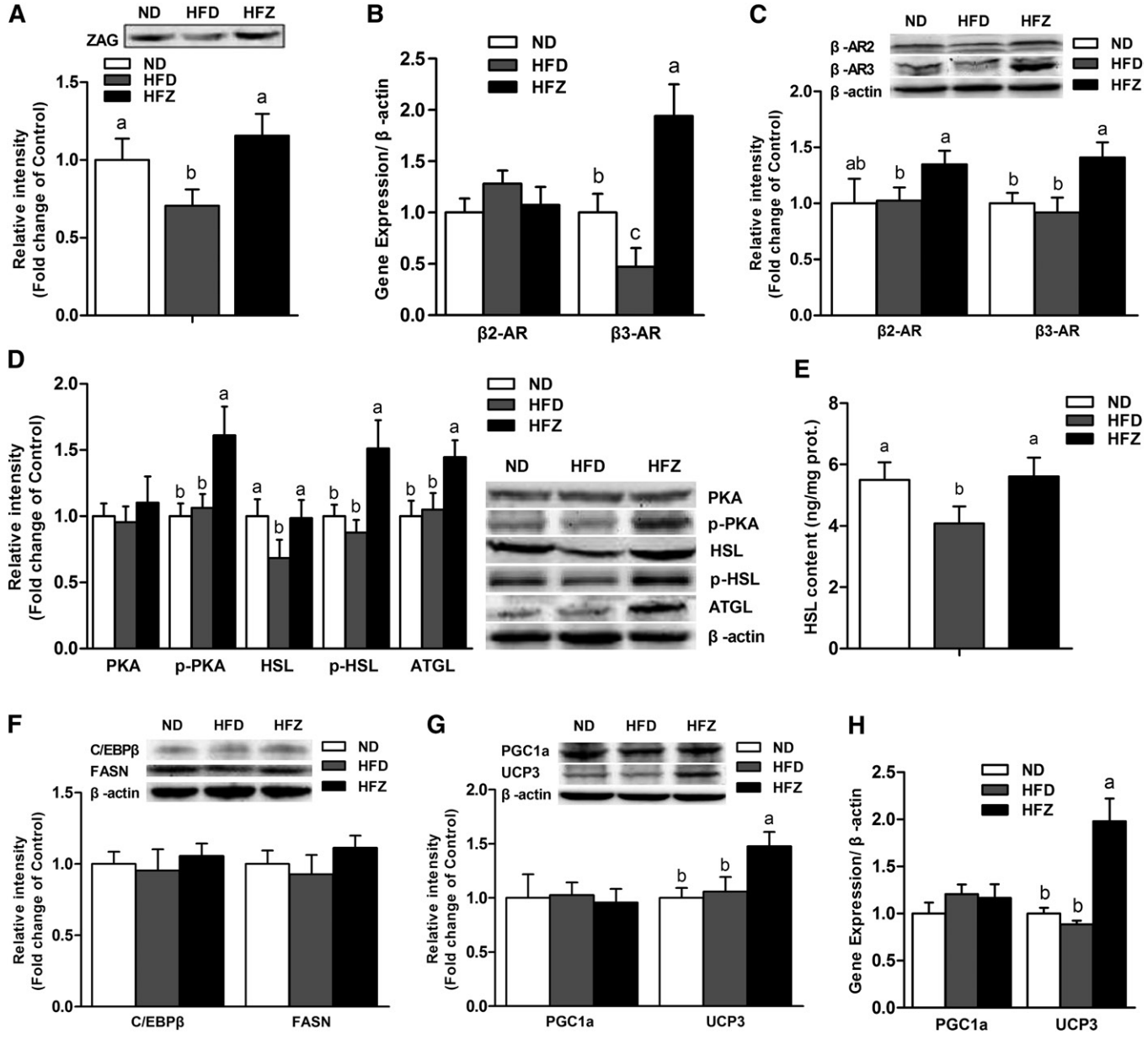

Fig. 4. ZAG overexpression increases lipolysis and UCP3 expression via the β-AR/cAMP/PKA pathway in skeletal muscle. A: Western blot analysis of ZAG in plasma of mice from the three groups (n = 6 per group). B: The mRNA expression of β2-AR and β3-AR (n = 6 per group). Western blot analysis revealed accumulation of β2-AR and β3-AR (C); PKA, HSL, p-HSL, and ATGL (D); and C/EBPβ and FASN (F) in the gastrocnemius muscle of mice from the three groups (n = 6 per group). HSL concentrations (E) in the gastrocnemius muscle of mice from the three groups (n = 6 per group). The Western blot analysis (G) and mRNA expression (H) of PGC1α and UCP3 in the gastrocnemius muscle of mice from the three groups (n = 6 per group). The ND group was fed with ND, whereas the HFD and HFZ groups were fed with HFD. Values are expressed as mean ± SEM. Different letters indicate significant differences between groups, as determined ($P < 0.05$). Error bars indicate SEM.

ZAG decreases intracellular lipid and promotes glucose uptake in C2C12 myotubes

In vitro, the intracellular TG concentrations were decreased by ZAG treatment both in BSA medium-cultured cells and in oleate-palmitate medium-cultured cells ($P < 0.05$, **Fig. 5A**). The intracellular NEFA concentrations showed no difference between the rZAG group and the control group (Fig. 5B). The intracellular HSL concentrations were increased in the rZAG group compared with the control group, both in BSA medium-cultured cells and in oleate-palmitate medium-cultured cells ($P < 0.05$, Fig. 5C). Glucose concentrations in the oleate-palmitate medium of the rZAG group were significantly lower compared with the counterpart control group ($P < 0.05$, Fig. 5D). These data indicate that ZAG treatment decreases intracellular lipid and promotes glucose uptake in C2C12 myotubes, especially in the oleate-palmitate-induced condition.

ZAG changes physiological parameters in HFD-induced obese mice

We investigated the physiological parameters related to energy homeostasis, such as VO2, VCO2, RER, feed intake,

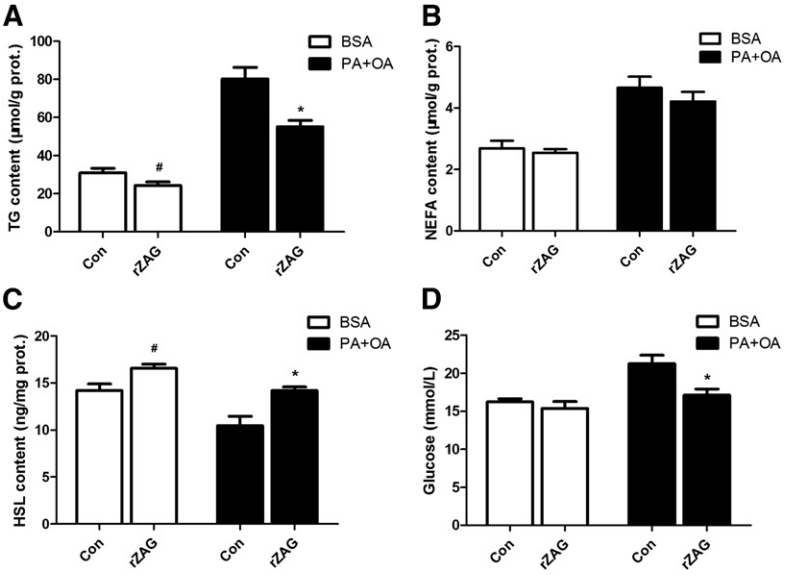

Fig. 5. ZAG decreases intracellular lipid and promotes glucose uptake in C2C12 myotubes. Concentrations of intracellular TG (A), intracellular NEFA (B), intracellular HSL (C), and cell medium glucose (D). The cells of the BSA group were cultured with 18.3% BSA alone, and the cells of PA+OA (palmitate-oleate) group were cultured with 1.0 mM oleate-palmitate solution. Values are expressed as mean ± SEM. Hash (#) denotes a significant difference ($P < 0.05$) between the rZAG group and the control (Con) group in normal cells. Asterisk (*) denotes a significant difference ($P < 0.05$) between the rZAG group and the control group in lipid accumulation cells. Error bars indicate SEM.

and heat production, among three groups. The results show that VO2, VCO2, RER, and heat production were observably lower ($P < 0.05$) in the HFD group than in the ND group, yet this decrease was significantly ($P < 0.05$) alleviated by the ZAG treatment (**Fig. 6**). These data suggest that ZAG overexpression increases energy consumption and carbohydrate utilization under HFD.

DISCUSSION

Obesity is considered a worldwide public-health crisis, affecting whole-body energy homeostasis, which can lead to insulin resistance, type II diabetes, and cardiovascular diseases. The adipose tissue is the body's largest energy reservoir and also an endocrine organ, which plays an important role in regulating energy homeostasis (20). ZAG, known as an important adipokine until now, has been shown to decrease the body weight and promote lipolysis in WAT (21, 22). Previous studies have demonstrated that ZAG has a negative correlation with obesity (23, 24). However, the function of ZAG on other tissue metabolism, except WAT, is still largely unknown. Here, we demonstrated that ZAG elicits stimulatory effects on insulin signaling in HFD-induced obese mice by decreasing lipid deposition in skeletal muscle.

In this study, insulin resistance was observed after 9 weeks on a HFD, which is indicated by the GTT and ITT curves (supplemental Fig. S1). The HOMA-IR was also significantly lower in the HFZ group compared with the HFD group, although no difference was observed in the basal blood glucose concentration. These results suggest that treatment with ZAG significantly improved the action of insulin. Skeletal muscle is the primary site of glucose disposal and insulin action. Insulin binds to the INSR leading to phosphorylation of the INSR. Phosphorylation of S307 is a well-known INSR site that affects IRS1 activity, and phosphorylation of S473 is an IRS1 site that affects AKT activity in the insulin signaling pathway. Once the INSR has been phosphorylated, glucose uptake is promoted by activating the IRS1/PI3K/AKT pathway (25). Our findings show that the mRNA expression levels of INSR, IRS1, GLUT1, and GLUT4 were increased by ZAG overexpression. Furthermore, the protein expression levels of p-IRS1, p-AKT, and M-Glut4 were also increased by ZAG overexpression. Consequently, these data indicate that ZAG overexpression can combat HFD-induced insulin resistance and activate the insulin signaling pathway and glucose uptake in skeletal muscle.

Previous in vitro studies have shown that ZAG acts directly to increase expression of UCP in BAT and skeletal muscle, which is likely to be directly related to the loss of adipose tissue (26). Administration of ZAG to ob/ob mice increases the expression of the β3-AR protein in BAT, WAT, and skeletal muscle (27). This study has also shown that treatment of HFD-induced obese mice with ZAG, increases the protein expression of β2-AR and β3-AR in skeletal muscle. It is well-known that activation of β-adrenergic receptors increases intracellular cAMP contents, and cAMP activates PKA. There are four phosphorylation sites within PKA: T197, S10, S139, and S338. In the present study, phosphor-T197 of PKA antibody was chosen to detect p-PKA levels. Phosphorylation of T197 in the activation loop is essential for activity. Changing T197 to alanine results in a folded but unstable and inactive protein (28). Other studies have shown that activation of the β2-AR/cAMP/PKA pathway can increase glucose uptake in skeletal muscle by promoting Glut4 translocation to the plasma membrane in an insulin-independent manner (29). When exercising or fasting, the insulin level is low and the β-AR/cAMP/PKA system is activated to promote catabolic processes to meet the energy demands of the skeletal muscle. In type II diabetes patients with insulin resistance, selective activation of PKA in skeletal muscle can serve as an alternative pathway for glucose disposal and glycemic control (30, 31).

Intramuscular fat is emerging as an important energy source during muscle contraction. Over the past two decades, there has been heavy emphasis on understanding the connection between intramuscular fat content and

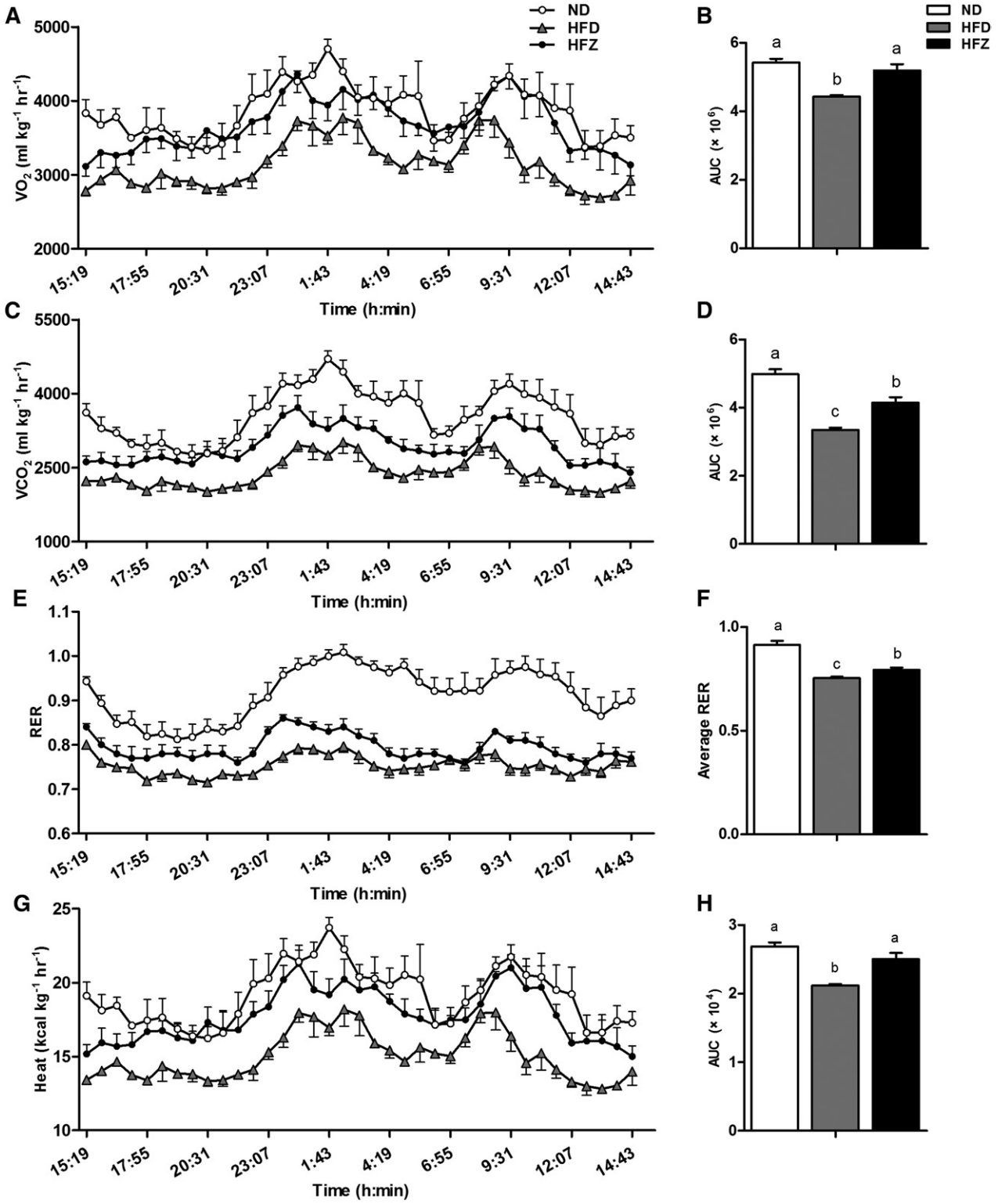

Fig. 6. ZAG overexpression restores physiological parameters. After the ZAG recombinant plasmid treatment, individually housed mice were monitored for VO2 (A) and its area under curve (AUC) (B), VCO2 (C) and its AUC (D), RER (E), average value of RER (F), and energy expenditure (G) and its AUC (H) among the three groups (n = 5 per group). Values are expressed as mean ± SEM. Different letters indicate significant differences between groups, as determined ($P < 0.05$). Error bars indicate SEM.

insulin action. Studies confirmed that elevated content of intramuscular fat is accompanied by higher availability of lipotoxic intermediates, which inhibit insulin signaling (8, 9, 32). In the present study, intramuscular fat was decreased significantly by the ZAG treatment compared with the HFD group. Fat mobilization from TG stores in tissues requires two major lipases, ATGL and HSL. ATGL catalyzes the initial step of TG hydrolysis and HSL is a rate-limiting enzyme

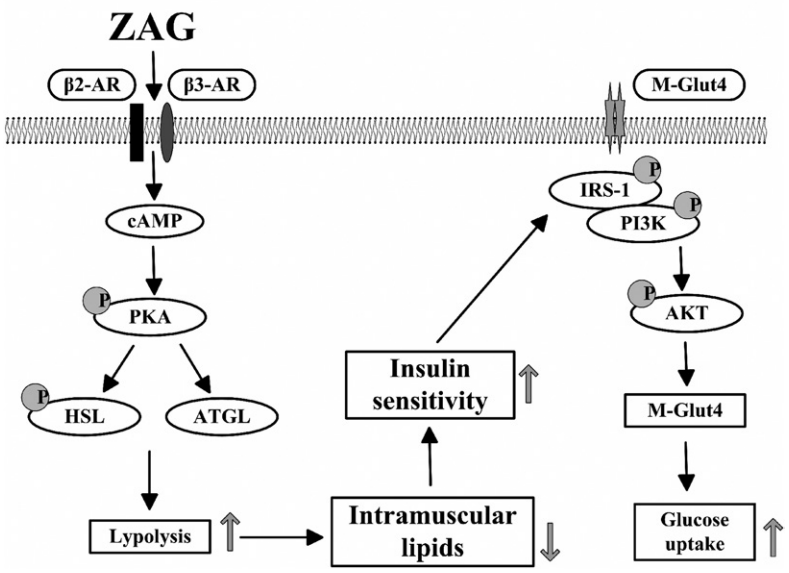

Fig. 7. Graphical summary of the study. The lipolytic effect of ZAG in skeletal muscle was attributed to the activation of β-AR and upregulation of cAMP via the β3-AR/cAMP/PKA pathway. The decrease of intramuscular lipids resulted in the increasing of insulin sensitivity and the promotion of glucose uptake.

responsible for hydrolyzing diacylglycerol to monoacylglycerol (33). The action of ZAG is associated with upregulated expression of lipolytic enzymes in adipose tissue of mice (12). In the present study, HSL protein levels and concentrations in the HFZ group were significantly higher than those in the HFD group. Meanwhile, lipolytic enzymes, such as p-HSL and ATGL, were significantly upregulated in the HFZ group. These results are in agreement with previous studies (12, 34). PKA activates HSL via promoting its phosphorylation. Previous works reveal that HSL contains three sites for PKA phosphorylation (S563, S659, and S660). As well, the site of p-HSL-S855 was chosen in the cAMP-PKA signaling pathway (35). In this study, phosphor-S855 of the HSL antibody was chosen to detect p-HSL levels.

In in vitro experiments, this study clearly showed that treatment with rZAG decreases intracellular lipid and promotes glucose uptake in C2C12 myotubes, although the NEFA levels were not different between the rZAG group and the control group. This probably resulted from increasing fatty acid utilization and mitochondrial β-oxidation. A previous study demonstrated that ZAG significantly promoted mitochondrial biogenesis accompanied by enhancement of lipid catabolism and fatty acid oxidation (36).

The RER is the ratio between the amount of carbon dioxide (CO2) produced by metabolism and oxygen (O2) used. A RER value of 0.7 indicates that fat is the predominant fuel source, a RER of 0.85 suggests a mix of fat and carbohydrates, and a RER value of 1 is indicative of carbohydrates being the predominant fuel source. In our study, the RER value was decreased significantly in the HFZ group compared with the HFD group in 24 h. This indicates that the ZAG treatment changed the energy metabolism pattern of the mice, and the treated mice utilized more carbohydrates for fuel.

The mRNA and protein expression levels of UCP3 were increased in the HFZ group, although no difference was observed in PGC1α expression. UCPs are located in the inner mitochondrial membrane and dissipate the stored energy as heat. These proteins are structurally related but with different distribution in various tissues. In skeletal muscle, UCP3 is a homolog of UCP1 and abundantly expressed (37). Postprandial thermogenesis has been associated with UCP3 and the futile calcium cycling (38). Some studies also showed that fatty acid transport and oxidation were obviously stimulated in UCP3-overexpressing mice in the skeletal muscle (39). Rising UCP3 expression in cultured human muscle stimulated fatty acid oxidation and usage (40). These reports suggest that UCP3 may be involved in fatty acid metabolism. In this study, heat production was higher in the HFZ group compared with the HFD group at every time point recorded within 24 h. Combined with the increased basal VO2 rate and carbon dioxide evolution rate in the HFZ group compared with the HFD group, these findings suggest that the body energy utilization was increased after the ZAG treatment.

In conclusion, this study provides evidence that ZAG alleviates obesity and improves insulin sensitivity in an HFD-induced obese mouse model. Furthermore, the present study revealed that this may be due to ZAG decreasing the lipid deposition in skeletal muscle (**Fig. 7**). However, further investigations are necessary to determine whether ZAG may influence the body's insulin signal through other pathways.

REFERENCES

1. Hoy, A. J., C. R. Bruce, S. M. Turpin, A. J. Morris, M. A. Febbraio, and M. J. Watt. 2011. Adipose triglyceride lipase-null mice are resistant to high-fat diet-induced insulin resistance despite reduced energy expenditure and ectopic lipid accumulation. *Endocrinology.* **152:** 48–58.
2. De Stefanis, D., R. Mastrocola, D. Nigro, P. Costelli, and M. Aragno. 2017. Effects of chronic sugar consumption on lipid accumulation and autophagy in the skeletal muscle. *Eur. J. Nutr.* **56:** 363–373.
3. Badin, P. M., I. K. Vila, K. Louche, A. Mairal, M. A. Marques, V. Bourlier, G. Tavernier, D. Langin, and C. Moro. 2013. High-fat diet-mediated lipotoxicity and insulin resistance is related to impaired lipase expression in mouse skeletal muscle. *Endocrinology.* **154:** 1444–1453.
4. de Lange, P., M. Moreno, E. Silvestri, A. Lombardi, F. Goglia, and A. Lanni. 2007. Fuel economy in food-deprived skeletal muscle: signaling pathways and regulatory mechanisms. *FASEB J.* **21:** 3431–3441.

5. Lee-Young, R. S., J. S. Bonner, W. H. Mayes, I. Iwueke, B. A. Barrick, C. M. Hasenour, L. Kang, and D. H. Wasserman. 2013. AMP-activated protein kinase (AMPK)α2 plays a role in determining the cellular fate of glucose in insulin-resistant mouse skeletal muscle. *Diabetologia.* **56:** 608–617.
6. Goodpaster, B. H., R. Theriault, S. C. Watkins, and D. E. Kelley. 2000. Intramuscular lipid content is increased in obesity and decreased by weight loss. *Metabolism.* **49:** 467–472.
7. Dobbins, R. L., L. S. Szczepaniak, B. Bentley, V. Esser, J. Myhill, and J. D. McGarry. 2001. Prolonged inhibition of muscle carnitine palmitoyltransferase-1 promotes intramyocellular lipid accumulation and insulin resistance in rats. *Diabetes.* **50:** 123–130.
8. Bachmann, O. P., D. B. Dahl, K. Brechtel, J. Machann, M. Haap, T. Maier, M. Loviscach, M. Stumvoll, C. A. Claussen, F. Schick, et al. 2001. Effects of intravenous and dietary lipid challenge on intramyocellular lipid content and the relation with insulin sensitivity in humans. *Diabetes.* **50:** 2579–2584.
9. Goodpaster, B. H., J. He, S. Watkins, and D. E. Kelley. 2001. Skeletal muscle lipid content and insulin resistance: Evidence for a paradox in endurance-trained athletes. *J. Clin. Endocrinol. Metab.* **86:** 5755–5761.
10. Bing, C., Y. Bao, J. Jenkins, P. Sanders, M. Manieri, S. Cinti, M. J. Tisdale, and P. Trayhurn. 2004. Zinc- 2-glycoprotein, a lipid mobilizing factor, is expressed in adipocytes and is up-regulated in mice with cancer cachexia. *Proc. Natl. Acad. Sci. USA.* **101:** 2500–2505.
11. Hirai, K., H. J. Hussey, M. D. Barber, S. A. Price, and M. J. Tisdale. 1998. Biological evaluation of a lipid-mobilizing factor isolated from the urine of cancer patients. *Cancer Res.* **58:** 2359–2365.
12. Gong, F. Y., S. J. Zhang, J. Y. Deng, H. J. Zhu, H. Pan, N. S. Li, and Y. F. Shi. 2009. Zinc-α2-glycoprotein is involved in regulation of body weight through inhibition of lipogenic enzymes in adipose tissue. *Int. J. Obes. (Lond.).* **33:** 1023–1030.
13. Rolli, V., M. Radosavljevic, V. Astier, C. Macquin, I. Castan-Laurell, V. Visentin, C. Guigne, C. Carpene, P. Valet, S. Gilfillan, et al. 2007. Lipolysis is altered in MHC class I zinc-alpha(2)-glycoprotein deficient mice. *FEBS Lett.* **581:** 394–400.
14. Russell, S. T., K. Hirai, and M. J. Tisdale. 2002. Role of beta 3-adrenergic receptors in the action of a tumour lipid mobilizing factor. *Br. J. Cancer.* **86:** 424–428.
15. Russell, S. T., and M. J. Tisdale. 2010. Antidiabetic properties of zinc-α2-glycoprotein in ob/ob mice. *Endocrinology.* **151:** 948–957.
16. Banks, A. S., F. E. McAllister, J. P. G. Camporez, P. J. H. Zushin, M. J. Jurczak, D. Laznik-Bogoslavski, G. I. Shulman, S. P. Gygi, and B. M. Spiegelman. 2015. An ERK/Cdk5 axis controls the diabetogenic actions of PPAR gamma. *Nature.* **517:** 391–395.
17. Wei, X., H. Song, L. Yin, M. G. Rizzo, R. Sidhu, D. F. Covey, D. S. Ory, and C. F. Semenkovich. 2016. Fatty acid synthesis configures the plasma membrane for inflammation in diabetes. *Nature.* **539:** 294–298.
18. Xu, M. Y., R. Chen, J. X. Yu, T. Liu, Y. Qu, and L. G. Lu. 2016. AZGP1 suppresses epithelial-to-mesenchymal transition and hepatic carcinogenesis by blocking TGFbeta1–ERK2 pathways. *Cancer Lett.* **374:** 241–249.
19. Delort, L., S. Perrier, V. Dubois, H. Billard, T. Mracek, C. Bing, M. P. Vasson, and F. Caldefie-Chézet. 2013. Zinc-α2-glycoprotein: a proliferative factor for breast cancer? In vitro study and molecular mechanisms. *Oncol. Rep.* **29:** 2025–2029.
20. Galic, S., J. S. Oakhill, and G. R. Steinberg. 2010. Adipose tissue as an endocrine organ. *Mol. Cell. Endocrinol.* **316:** 129–139.
21. Russell, S. T., and M. J. Tisdale. 2011. Studies on the antiobesity effect of zinc-alpha2-glycoprotein in the ob/ob mouse. *Int. J. Obes. (Lond.).* **35:** 345–354.
22. Russell, S. T., and M. J. Tisdale. 2011. Studies on the anti-obesity activity of zinc-alpha(2)-glycoprotein in the rat. *Int. J. Obes. (Lond.).* **35:** 658–665.
23. Liu, M., H. Zhu, Y. Dai, H. Pan, N. Li, L. Wang, H. Yang, K. Yan, and F. Gong. 2018. Zinc-alpha2-glycoprotein is associated with obesity in Chinese people and HFD-induced obese mice. *Front. Physiol.* **9:** 62.
24. Mracek, T., Q. Ding, T. Tzanavari, K. Kos, J. Pinkney, J. Wilding, P. Trayhurn, and C. Bing. 2010. The adipokine zinc-α2-glycoprotein (ZAG) is downregulated with fat mass expansion in obesity. *Clin. Endocrinol. (Oxf.).* **72:** 334–341.
25. Tanti, J. F., T. Grémeaux, E. Van Obberghen, and Y. Le Marchand-Brustel. 1994. Insulin receptor substrate 1 is phosphorylated by the serine kinase activity of phosphatidylinositol 3-kinase. *Biochem. J.* **304:** 17–21.
26. Sanders, P. M., and M. J. Tisdale. 2004. Effect of zinc-alpha2-glycoprotein (ZAG) on expression of uncoupling proteins in skeletal muscle and adipose tissue. *Cancer Lett.* **212:** 71–81.
27. Russell, S. T., and M. J. Tisdale. 2012. Role of beta-adrenergic receptors in the anti-obesity and anti-diabetic effects of zinc-alpha2-glycoprotien (ZAG). *Biochim. Biophys. Acta.* **1821:** 590–599.
28. Langer, T., M. Vogtherr, B. Elshorst, M. Betz, U. Schieborr, K. Saxena, and H. Schwalbe. 2004. NMR backbone assignment of a protein kinase catalytic domain by a combination of several approaches: application to the catalytic subunit of cAMP-dependent protein kinase. *ChemBioChem.* **5:** 1508–1516.
29. Yang, H., and L. Yang. 2016. Targeting cAMP/PKA pathway for glycemic control and type 2 diabetes therapy. *J. Mol. Endocrinol.* **57:** R93–R108.
30. Sato, M., N. Dehvari, A. I. Oberg, O. S. Dallner, A. L. Sandstrom, J. M. Olsen, R. I. Csikasz, R. J. Summers, D. S. Hutchinson, and T. Bengtsson. 2014. Improving type 2 diabetes through a distinct adrenergic signaling pathway involving mTORC2 that mediates glucose uptake in skeletal muscle. *Diabetes.* **63:** 4115–4129.
31. Ngala, R. A., J. F. O'Dowd, C. J. Stocker, M. A. Cawthorne, and J. R. S. Arch. 2013. β2-adrenoceptor agonists can both stimulate and inhibit glucose uptake in mouse soleus muscle through ligand-directed signalling. *Naunyn Schmiedebergs Arch. Pharmacol.* **386:** 761–773.
32. Bosma, M., S. Kersten, M. K. C. Hesselink, and P. Schrauwen. 2012. Re-evaluating lipotoxic triggers in skeletal muscle: Relating intramyocellular lipid metabolism to insulin sensitivity. *Prog. Lipid Res.* **51:** 36–49.
33. Schweiger, M., R. Schreiber, G. Haemmerle, A. Lass, C. Fledelius, P. Jacobsen, H. Tornqvist, R. Zechner, and R. Zimmermann. 2006. Adipose triglyceride lipase and hormone-sensitive lipase are the major enzymes in adipose tissue triacylglycerol catabolism. *J. Biol. Chem.* **281:** 40236–40241.
34. Chu, X., X. He, Z. P. Shi, C. J. Li, F. C. Guo, S. T. Li, Y. Li, L. X. Na, and C. H. Sun. 2015. Ursolic acid increases energy expenditure through enhancing free fatty acid uptake and β-oxidation via an UCP3/AMPK-dependent pathway in skeletal muscle. *Mol. Nutr. Food Res.* **59:** 1491–1503.
35. Xiong, Y., Z. Qu, N. Chen, H. Gong, M. Song, X. Chen, J. Du, and C. Xu. 2014. The local corticotropin-releasing hormone receptor 2 signalling pathway partly mediates hypoxia-induced increases in lipolysis via the cAMP–protein kinase A signalling pathway in white adipose tissue. *Mol. Cell. Endocrinol.* **392:** 106–114.
36. Xiao, X. H., X. Y. Qi, Y. D. Wang, L. Ran, J. Yang, H. L. Zhang, C. X. Xu, G. B. Wen, and J. H. Liu. 2018. Zinc alpha2 glycoprotein promotes browning in adipocytes. *Biochem. Biophys. Res. Commun.* **496:** 287–293.
37. Boss, O., S. Samec, A. Paoloni-Giacobino, C. Rossier, A. Dulloo, J. Seydoux, P. Muzzin, and J. P. Giacobino. 1997. Uncoupling protein-3: a new member of the mitochondrial carrier family with tissue-specific expression. *FEBS Lett.* **408:** 39–42.
38. Fuller-Jackson, J. P., and B. A. Henry. 2018. Adipose and skeletal muscle thermogenesis: studies from large animals. *J. Endocrinol.* **237:** R99–R115.
39. Bezaire, V., L. L. Spriet, S. Campbell, N. Sabet, M. Gerrits, A. Bonen, and M. E. Harper. 2005. Increased fatty acid oxidation in transgenic mice overexpressing UCP3 in skeletal muscle. *FASEB J.* **19:** 977–979.
40. García-Martinez, C., B. Sibille, G. Solanes, C. Darimont, K. Macé, F. Villarroya, and A. M. Gómez-Foix. 2001. Overexpression of UCP3 in cultured human muscle lowers mitochondrial membrane potential, raises ATP/ADP ratio, and favors fatty acid vs. glucose oxidation. *FASEB J.* **15:** 2033–2035.